


 Cite this: *RSC Adv.*, 2018, **8**, 13474

 Received 29th January 2018  
 Accepted 3rd April 2018

 DOI: 10.1039/c8ra00894a  
[rsc.li/rsc-advances](http://rsc.li/rsc-advances)

## Facile preparation of epoxy based elastomers with tunable $T_{gs}$ and mechanical properties

 Bin Chen,<sup>\*a</sup> Jingyu Li,<sup>ab</sup> Tong Liu,<sup>ab</sup> Zhendong Dai<sup>b</sup> and Haichao Zhao <sup>b</sup>

In this work, a secondary amine-capped polyaspartic ester (PAE-D230) was synthesized using diethyl maleate and amine-terminated polyether (D230) *via* Michael addition reaction. By modulating the molar ratio of preliminary amine containing D230 and secondary amine-capped PAE-D230 during the curing process with epoxy precursor **E44**, we obtained epoxy shape memory polymers with tunable  $T_{gs}$  (−12–20 °C), controllable mechanical properties with tensile stress from 0.8 to 14.1 MPa, tensile modulus from 0.7 to 872.0 MPa, and elongation at break from 45.2 to 195.1%. The influence of the composition of curing components on the thermal properties, thermomechanical, mechanical properties, shape memory effect were systematically studied by DSC, TGA, DMA, tensile-stress measurements.

### 1. Introduction

Epoxy resins, a highly crosslinked network cured with a variety of hardeners such as amines,<sup>1</sup> anhydrides,<sup>2</sup> thiols<sup>3</sup> and imidazoles,<sup>4</sup> have many industrial applications owing to their excellent properties on mechanical strength,<sup>5</sup> strong adhesion,<sup>6</sup> chemical resistance<sup>7</sup> and high electrical resistance.<sup>8</sup> However, the high crosslinked epoxy network usually suffers from their inherent brittleness, low impact strength and low elongation at break,<sup>9,10</sup> which limited their further applications. Recently, epoxy-based shape memory polymers (SMPs)<sup>11–14</sup> with relatively high failure strains and modulus have drawn a lot of research interest because their unique properties compared to traditional SMPs such as high dimensional stability, non-volatile monomers and ease of processing.

A general strategy to obtain epoxy SMPs is to incorporate soft segment in the epoxy crosslinked network or reduce the crosslink density.<sup>15–19</sup> For typical instance, Xie *et al.* reported the preparation of epoxy SMPs by modulating the ratio of rigid aromatic diepoxy and soft aliphatic diepoxy during the curing process with aliphatic diamine. Although the  $T_{gs}$  could be tuned in a wide temperature range (25–100 °C), the elongation at break was less than 30% owing to its inherent crosslink density.<sup>20</sup> Leonardi *et al.* reported the curing reaction of an aromatic diepoxy with an aromatic diamine and a alkylamine achieve the epoxy network with both chemical and physical crosslinking, possessing a shape memory behavior with a  $T_g$

about 40 °C and the elongation at break as high as 75%.<sup>21</sup> Zheng *et al.* demonstrated the preparation of two component epoxy-amine system by tuning the molar ratio of epoxy **E44** and Jeffamine D230, achieving a series of shape memory polymers with tunable  $T_{gs}$  (40–80 °C), high strain, excellent shape fixity, recovery ability and cycling stability. Despite the great progress of epoxy SMPs, a major drawback is their relative high  $T_g$  (>25 °C),<sup>22</sup> low tensile stress and low strain at break, which limited their potential applications as lower temperature. Therefore, the development of epoxy based SMPs with desirable properties still remains challenge.

In this work, a secondary amine-capped polyaspartic ester (PAE-D230) was synthesized using diethyl maleate and amine-terminated polyether (D230) *via* Michael addition reaction (Fig. 1). By modulating the molar ratio of preliminary amine containing D230 and secondary amine-capped PAE-D230 during the curing process with epoxy precursor **E44**, we obtained epoxy shape memory polymers with tunable  $T_{gs}$  (−12–20 °C), controllable mechanical properties with tensile stress from 0.8 to 14.1 MPa, tensile modulus from 0.7 to 872.0 MPa, and elongation at break from 45.2 to 195.1%. The influence of the composition of curing components on the thermal properties, thermo-mechanics, mechanical properties, shape memory effect were systematically studied by DSC, TGA, DMA, tensile-stress measurements.

### 2. Experimental

#### 2.1 Materials

Epoxy resin (**E44**, epoxy value 0.44) was provided by Jining Baichuan Chemical Co., Ltd., China. Curing agent poly(propylene glycol)bis(2-aminopropyl ether) (Jeffamine D230) and diethyl maleate (DEM, 96%) were purchased from Shanghai Aladdin Bio-Chem Technology Co., Ltd.

<sup>a</sup>School of Materials Science and Engineering, Shenyang University of Chemical Technology, 11 St. Economic & Technological Development Zone, Shenyang 110142, P. R. China. E-mail: bchen63@163.com

<sup>b</sup>Key Laboratory of Marine Materials and Related Technologies, Zhejiang Key Laboratory of Marine Materials and Protective Technologies, Ningbo Institute of Materials Technology and Engineering, Chinese Academy of Sciences, Ningbo 315201, P. R. China. E-mail: zhaohaichao@nimte.ac.cn



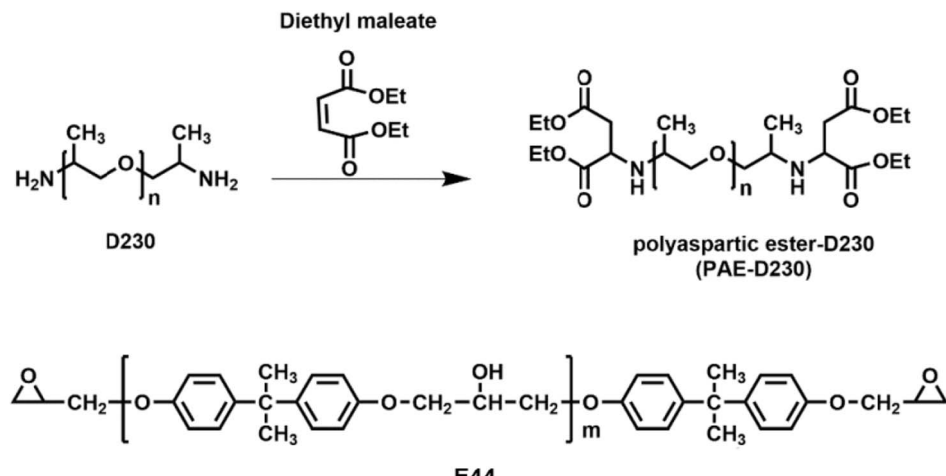


Fig. 1 Chemical structures of epoxy resin and amine-terminated curing agent.

## 2.2 Synthesis of PAE-D230

In a typical experiment, D230 was first dried in a vacuum oven at 80 °C for 4 h, then the 172.18 g of DEM (1 mol) was slowly added to 115 g of D230 (0.5 mol) under nitrogen protection environment and the temperature was controlled below 60 °C during the dropwise addition process, and the reaction was continued at 80 °C for 20 h. For complete Michael addition reaction, the mixtures were kept at room temperature for one month to obtain a transparent pale yellow liquid (PAE-D230) with the  $M_n$  of 570 g mol<sup>-1</sup>.

## 2.3 Preparation of epoxy shape memory polymer material

The formulation recipes of E44, PAE-D230, and D230 was summarized in Table 1. For every case, the mixtures were mechanically stirred for 20 min followed by degassing in a vacuum oven at 50 °C for 20 min to remove the bubbles. The curing reaction was conducted at 80 °C for 2 h and 120 °C for 8 h

in Teflon mold. For comparison purpose, a series of soft epoxy based elastomer materials were successful prepared, the cured sample was molded rectangular samples and cut into dog bones for further tensile testing and dynamic mechanical analysis, respectively.

## 2.4 Instruments and characterization

Intelligent Fourier infrared (FTIR) and Micro-FTIR spectra were obtained by NICOLET 6700 spectrometer and Agilent Cary 660/620 spectrometer. Tensile test was performed under ambient conditions according to ASTM 638 using Universal Machine model INSTRON 5869 with the crosshead speed of 5 mm min<sup>-1</sup>, values were converted to stress-strain and a Young's modulus was calculated from the initial slope 5 parallel samples were measured and averaged. Thermal analysis of the epoxy shape memory polymer materials were performed by Netisch thermo gravimetric analysis (TGA), the temperature ranged from 30 to 800 °C at a heating rate of 10 °C min<sup>-1</sup> under air atmosphere to examine the thermal degradation behavior. The DSC measurement was conducted on a METTLER TOLEDO-TGA/DSC I under a nitrogen atmosphere and at a heating rate of 20 °C min<sup>-1</sup>, the temperature ranged from -40 to 70 °C. Dynamic mechanical analysis (DMA) were performed on DMAQ800, and the rectangular samples (25 × 6.5 × 1.5 mm) were heated at a heating rate of 3.00 °C min<sup>-1</sup>, amplitude 2 μm, frequency 1 Hz.

Table 1 Formulation of epoxy based elastomer

Samples	Components (molar ratio)		
	E44	PAE-D230	D230
1	100	80	10
2	100	80	20
3	100	80	30
4	100	80	40
5	100	80	50
6	100	60	10
7	100	60	20
8	100	60	30
9	100	60	40
10	100	60	50
11	100	40	10
12	100	40	20
13	100	40	30
14	100	40	40
15	100	40	50

## 3. Result and discussion

### 3.1 Preparation of epoxy based elastomer

The starting materials D230, PAE-D230 were characterized by FTIR spectra, as shown in Fig. 2. D230 showed typical -NH<sub>2</sub> stretching vibrations at 3260 and 3288 cm<sup>-1</sup>,<sup>23,24</sup> and the strong characteristic band at 1108 cm<sup>-1</sup> was related to aliphatic ether of polyetheramine. The PAE-D230 was obtained from Michael addition reaction of D230 and DEM. The disappearance of -NH<sub>2</sub> absorption bands and the presence of new bands at 3333 cm<sup>-1</sup> (secondary amine), 1736 and 765 cm<sup>-1</sup> (O-C=O vibrations)



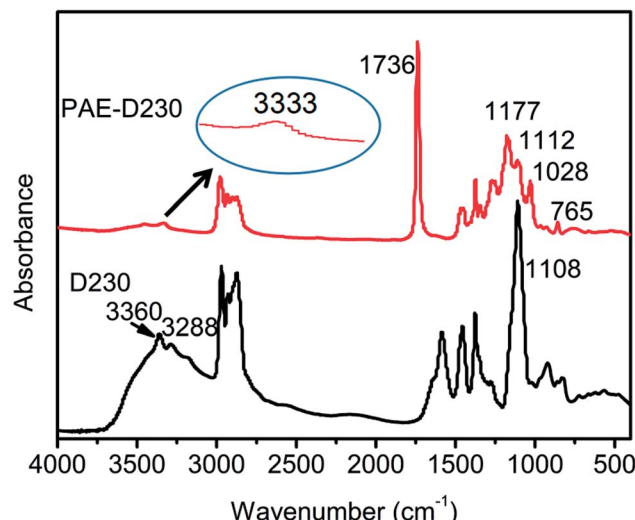


Fig. 2 FTIR spectra of PAE-D230 and the D230.

confirmed the successful synthesis of PAE-230. The bands found for 1177, 1112, and 1028  $\text{cm}^{-1}$  were due to the aliphatic ether, implying that the successfully reaction between D230 and DEM. A band at 1736  $\text{cm}^{-1}$  of cured network was attributed to O=C=O stretching vibration, which proved the existence of the ester structure.

Conventionally, epoxy based SMPs could be obtained by modulating the crosslinking density of cured network. In present work, we explore a secondary amine-capped poly-aspartic ester (PAE-D230) and primary amine containing D230 as hardener, curing reaction of epoxy E44, PAE-D230 and D230 as predesigned compositions at 80  $^{\circ}\text{C}$  for 2 h and 120  $^{\circ}\text{C}$  for 8 h afforded the corresponding elastic epoxy resin with shape memory effect.

### 3.2 Thermal properties of epoxy based elastomer

The thermal stability of cured epoxy E44, PAE-D230 and D230 formulations were analyzed by TGA and DSC analysis. Studying

the degradation of epoxy resins, has been an object of constant research.<sup>25-28</sup> The information obtained by the controlled degradation of the polymer can be used to evaluate whether a given material will be useful for a high temperature potential application. Fig. 3 showed the TGA and DTG curves of cured specimens. The weight loss rate of the sample at different temperatures was calculated from the difference between the weight percent of the initial weight of the sample and the weight percentage of the sample at the corresponding temperature. From an overall point of view, the thermal stability of each group of samples (E44 : PAE-D230 : D230 = 100 : 80 : 10–50, 100 : 60 : 10–50, 100 : 40 : 10–50) decreased with the increase of the feed ratio of D230. This may be due to the gradual excess of active hydrogen on the amino groups in the entire curing system. And the excessive amounts of D230 played a role as plasticizer in the system. No obvious weight loss was found from room temperature to 200  $^{\circ}\text{C}$ . For ease of comparison, the temperature ( $T_{d20}$  and  $T_{d80}$ ) of each test material weight loss rate reached 20 wt% and 80 wt% were listed in Table 2. As can be seen, the  $T_{d20}$  s of the as prepared polymers ranged from 259  $^{\circ}\text{C}$  to 366  $^{\circ}\text{C}$ , and the  $T_{d80}$  s ranged from 442  $^{\circ}\text{C}$  to 406  $^{\circ}\text{C}$ . According to the DTG curves, there were two thermal degradation stages identified from 200 to 500  $^{\circ}\text{C}$  of almost all the samples except for formulations with E-44 : PAE-D230 : D230 = 100 : 60 : 30. The weight loss of first degradation stage from 200 to 330  $^{\circ}\text{C}$  (the peak of DTG appears at the temperature range of 253 to 283  $^{\circ}\text{C}$ ), which were corresponded to the decomposition of ester groups of PAE-D230 and the epoxy network with a low crosslinked density.<sup>29</sup> Ester groups are thermally cleavable by a  $\beta$ -elimination mechanism.<sup>30,31</sup> The weight loss of the second groups from 330 to 500  $^{\circ}\text{C}$  (the peak of DTG appears at the temperature range of 375 to 397  $^{\circ}\text{C}$ ), which were attributed the degradation of high crosslinked epoxy network.<sup>32,33</sup>

The effects of feed ratio of PAE-D230/D230 on the glass transition temperature of the resulting elastomers were examined by DSC. As shown the DSC thermograms of the specimens in Fig. 4 and  $T_g$ s were tabulated in Table 3, the  $T_g$ s of all the

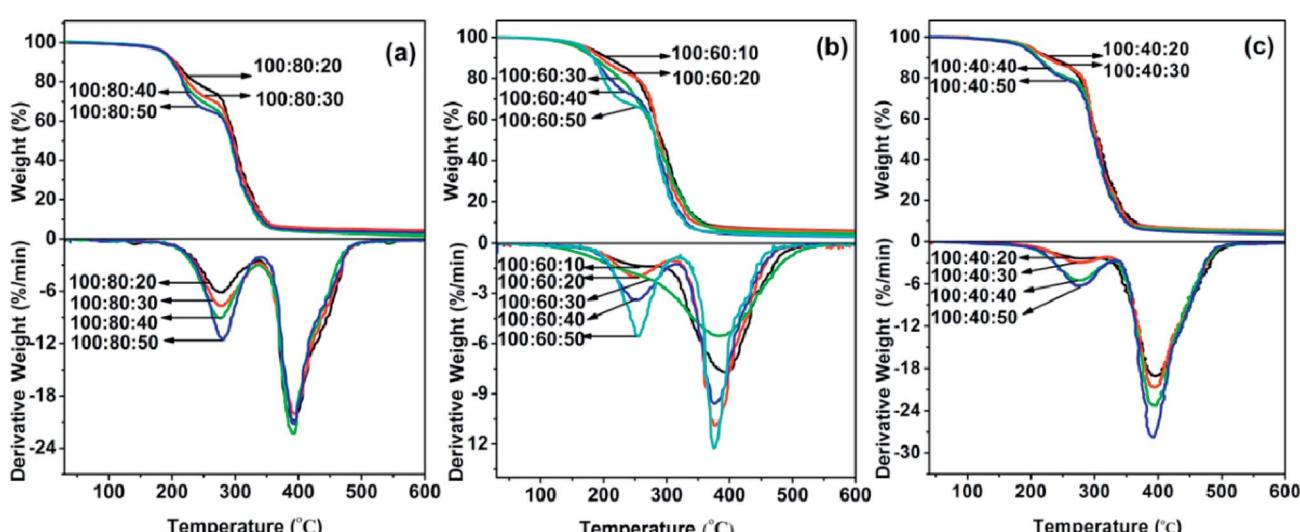


Fig. 3 Thermo-gravimetric curves and derivative weight curves of shape memory epoxy.



Table 2  $T_{d20}$  and  $T_{d80}$  and DTG peaks of shape memory epoxy

E44 : PAE-D230 : D230	$T_{d20}/^{\circ}\text{C}$	$T_{d80}/^{\circ}\text{C}$	DTG peaks/ $^{\circ}\text{C}$
100 : 80 : 10	—	—	—
100 : 80 : 20	309	441	282 395
100 : 80 : 30	293	432	279 395
100 : 80 : 40	283	425	277 393
100 : 80 : 50	284	422	281 393
100 : 60 : 10	331	433	276 394
100 : 60 : 20	332	422	253 378
100 : 60 : 30	294	432	— 385
100 : 60 : 40	271	409	260 375
100 : 60 : 50	259	406	253 376
100 : 40 : 10	—	—	—
100 : 40 : 20	366	442	283 397
100 : 40 : 30	362	440	276 394
100 : 40 : 40	323	431	276 397
100 : 40 : 50	334	435	275 391

sample were varied between  $-12$  and  $20$   $^{\circ}\text{C}$ , illustrated that the prepared epoxy networks were rubbery at room temperature and the working temperature range of the elastomer could be

tuned by adjusting the ratio of PAE-D230 : D230. Moreover, the E44/PAE-D230/D230 ratio has significant impact on the  $T_{\text{g}}$ s of the obtained elastomer. For the samples with rich PAE-D230 (100 : 80 : 10–50), the  $T_{\text{g}}$ s are observed to vary between  $-3$  and  $-12$   $^{\circ}\text{C}$ , while the  $T_{\text{g}}$ s changed to the region of  $-3$ – $19$   $^{\circ}\text{C}$  and  $13$ – $20$   $^{\circ}\text{C}$  for formulations with less PAE-D230 (100 : 60 : 10–50, 100 : 40 : 10–50), indicated that the decrease in PAE-D230 led to the increase in crosslink density and the resulting glass transition temperature of the samples.

Glass transition temperature generally refers to the temperature that the polymer from high-elastic state changes to glassy state, which does not have a fixed value.  $T_{\text{g}}$  value is related to the method of measurement and conditions. When the polymer undergoes a glass transition, the heat capacity of polymer suddenly changes. The DSC curve shows an abrupt change in the direction of the base line toward the endothermic direction, from which the  $T_{\text{g}}$  of the polymer can be determined. The dynamic mechanical response of a polymer material is obtained by applying a sinusoidal alternating load on the polymer under DMA test. Although the  $T_{\text{g}}$ s values measured from DSC and DMA are different, but they exhibited the same trend in this work.

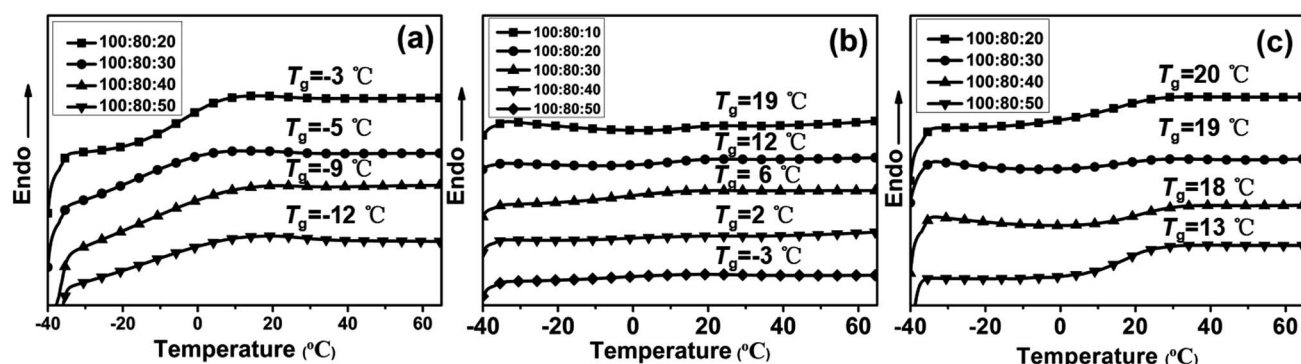


Fig. 4 DSC curves of shape memory epoxy.

Table 3 The thermal performance of shape memory epoxy

E44 : PAE-D230 : D230	$T_{\text{g}}$ by DSC ( $^{\circ}\text{C}$ )	$T_{\text{g}}$ by DMA ( $^{\circ}\text{C}$ )	$\tan \delta_{\text{max}}$	$\Delta T$ at $\tan \delta > 0.3$ ( $^{\circ}\text{C}$ )
100 : 80 : 10	—	—	—	—
100 : 80 : 20	-3	29	1.56	42
100 : 80 : 30	-5	24	1.30	42
100 : 80 : 40	-9	21	0.99	41
100 : 80 : 50	-12	19	0.97	36
100 : 60 : 10	19	36	1.80	51
100 : 60 : 20	12	35	1.51	40
100 : 60 : 30	6	30	1.30	38
100 : 60 : 40	2	28	1.04	38
100 : 60 : 50	-3	24	1.03	37
100 : 40 : 10	—	—	—	—
100 : 40 : 20	20	47	1.50	42
100 : 40 : 30	19	41	1.38	34
100 : 40 : 40	18	38	1.24	33
100 : 40 : 50	13	34	1.15	32



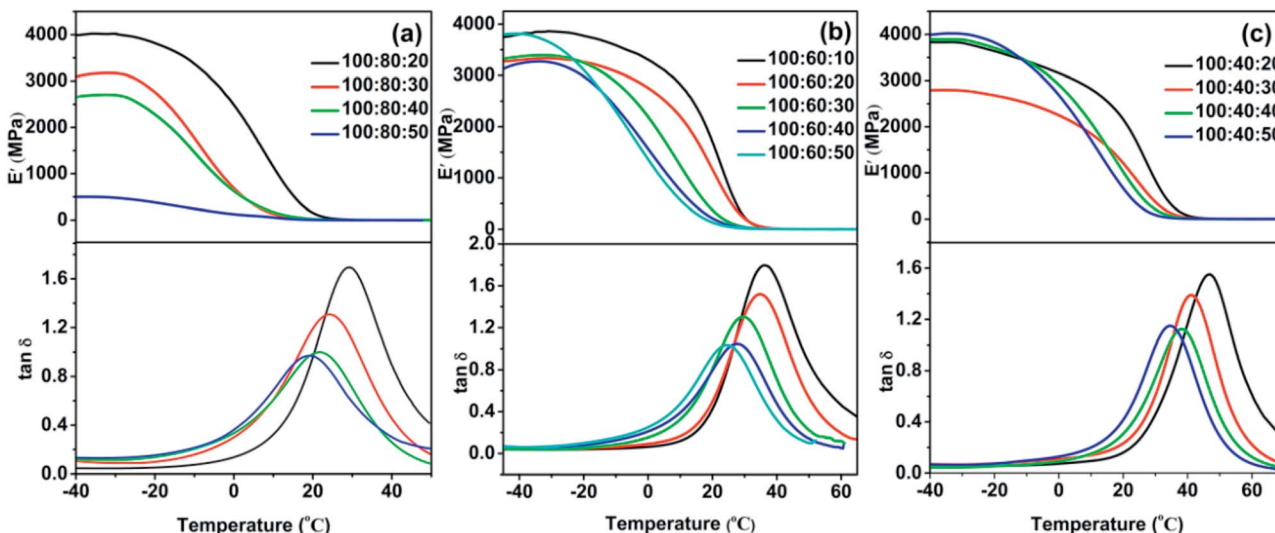


Fig. 5 Temperature dependence of storage modulus and loss factor of the shape memory epoxy.

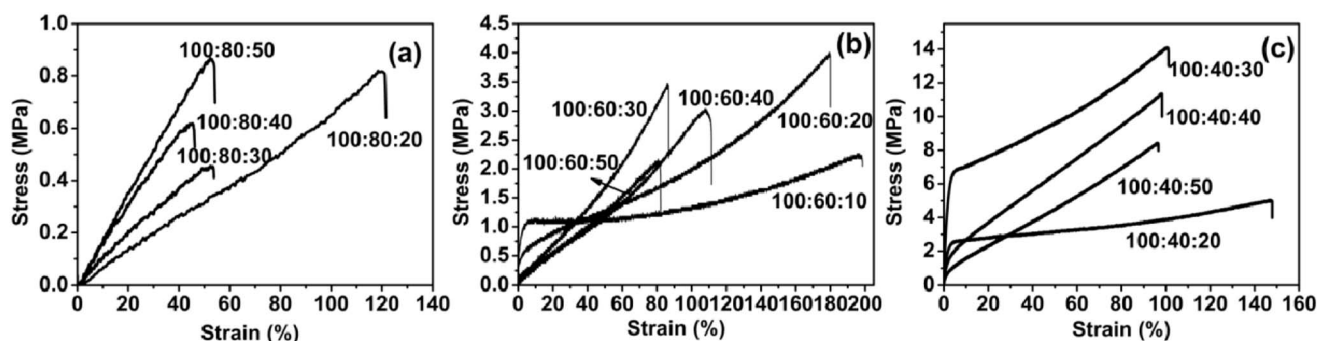


Fig. 6 Stress-strain curves of shape memory epoxy.

### 3.3 Dynamic thermomechanical analysis (DMA) analysis

The visco-elastic properties and damping behavior of cured samples were examined using DMA. Fig. 5 showed the temperature dependence of storage modulus ( $E'$ ) and loss factor ( $\tan \delta$ ) for the cured elastomers. All samples exhibited temperature dependent visco-elastic properties, showed high storage modulus at glass state and low  $E'$  in the rubbery state. Moreover, the ratio of curing agent (PAE-D230 : D230) had also a significant effect on storage modulus of the obtained elastomer. For instance, the sample with the composition of 100 : 80 : 20 (Fig. 5a) has a  $E'$  of 3993 MPa at  $-40\text{ }^{\circ}\text{C}$  and 2481 MPa at  $0\text{ }^{\circ}\text{C}$ , yet the  $E'$  decreased to 499 MPa at  $-40\text{ }^{\circ}\text{C}$  and 126 MPa at  $0\text{ }^{\circ}\text{C}$  with the high ratio of PAE-D230 : D230 (100 : 80 : 50). As shown in Table 3, the  $T_g$ s determined by the peaks of  $\tan \delta$  are in the range of  $19\text{--}47\text{ }^{\circ}\text{C}$ , which differed from the data from DSC but showed the similar trend.<sup>23</sup> On the other hand, the maximum peak value of  $\tan \delta$  varied from 0.97 to 1.80 and  $\Delta T$  ( $\tan \delta$  higher than 0.3) varied from  $32\text{ }^{\circ}\text{C}$  to  $51\text{ }^{\circ}\text{C}$ , displayed excellent and tunable dimpling behavior.

### 3.4 Mechanical properties

The tensile properties of the PAE-D230/D230 cured elastomer were determined by stress-strain measurements. Typical strain-stress plots were shown in Fig. 6, and the tensile properties, including tensile strength, Young's modulus and elongation-to-break has been given in Table 4.

The samples of 100 : 80 : 10 and 100 : 40 : 10 could not be solidified, so there was no mechanical performance data. The mechanical properties of the elastomer sample were related to the amount of active hydrogen on the amino group in the reactant system, which depend on the feed of D230 and PAE-D230. Due to the large molecular weight of PAE-D230, it appeared that the mechanical properties of the elastomer increased with the decrease in PAE-D230 content. For each group of elastomers with the fixed amount of E-44-D230, mechanical properties were related to the feed of D230. With the increase in the amount of D230, the amount of active hydrogen atoms on the amino group in the system had undergone a process from insufficient to excessive. The group of E-44 : PAE-D230 : D230 = 100 : 40 : 10–50 clearly conforms to this rule. The rules for the mechanical properties of the elastomer

Table 4 Tensile properties of shape memory epoxy

E44 : PAE-D230 : D230 (molar ratio)	Tensile strength (MPa)	Tensile modulus (MPa)	Elongation at break (%)
100 : 80 : 10	—	—	—
100 : 80 : 20	0.8 ± 0.2	0.7 ± 0.3	119.6 ± 7.5
100 : 80 : 30	0.5 ± 0.1	1.0 ± 0.2	53.4 ± 5.3
100 : 80 : 40	0.6 ± 0.2	1.6 ± 0.2	45.2 ± 5.0
100 : 80 : 50	0.9 ± 0.3	1.8 ± 0.3	52.6 ± 3.7
100 : 60 : 10	2.2 ± 0.5	318.8 ± 20.9	195.1 ± 8.5
100 : 60 : 20	3.9 ± 0.3	167.2 ± 22.5	178.7 ± 10.2
100 : 60 : 30	3.0 ± 0.6	69.1 ± 12.1	106.6 ± 6.8
100 : 60 : 40	3.4 ± 0.3	47.5 ± 8.2	86.6 ± 5.0
100 : 60 : 50	2.1 ± 0.2	30.3 ± 5.8	81.0 ± 5.9
100 : 40 : 10	—	—	—
100 : 40 : 20	5.0 ± 0.8	782.2 ± 59.4	147.0 ± 11.8
100 : 40 : 30	14.1 ± 1.2	872.0 ± 65.8	100.4 ± 9.5
100 : 40 : 40	11.3 ± 1.8	535.5 ± 44.3	98.6 ± 4.3
100 : 40 : 50	8.4 ± 1.0	302.0 ± 32.7	96.4 ± 5.0

groups (E-44 : PAE-D230 : D230 = 100 : 80 : 10–50 and 100 : 60 : 10–50) may be related to the amount of PAE-D230. For the samples with rich PAE-D230 (100 : 80 : 10–50), the tensile strength is observed to varies between 0.5–0.9 MPa, while the tensile modulus changed to the region of 0.7–1.8 MPa and the elongation at break of 45.2–119.6%. For the formulations with PAE-D230 (100 : 60 : 10–50), the tensile strength is observed to be varied between 2.1–3.9 MPa. As the ratio of E44 and D230 decreased from 100 : 10 to 100 : 50, the tensile modulus (318.8–30.3 MPa) and elongation at break (195.1–81.0%) went down

dramatically. Therefore, the tensile strength value significantly decreased with the increased in molar ratio of the D230 and elongation at break follows a same trend as the tensile strength. The tensile strength is observed to vary between 5.0 and 14.1 MPa, the tensile modulus changed to the region of 302.0–872.0 MPa and elongation at break of 96.4–147.0%, respectively, for formulations with less PAE-D230 (100 : 40 : 10–50). The above results had indicated that the decrease in PAE-D230 led to the increased in tensile strength and tensile modulus of the

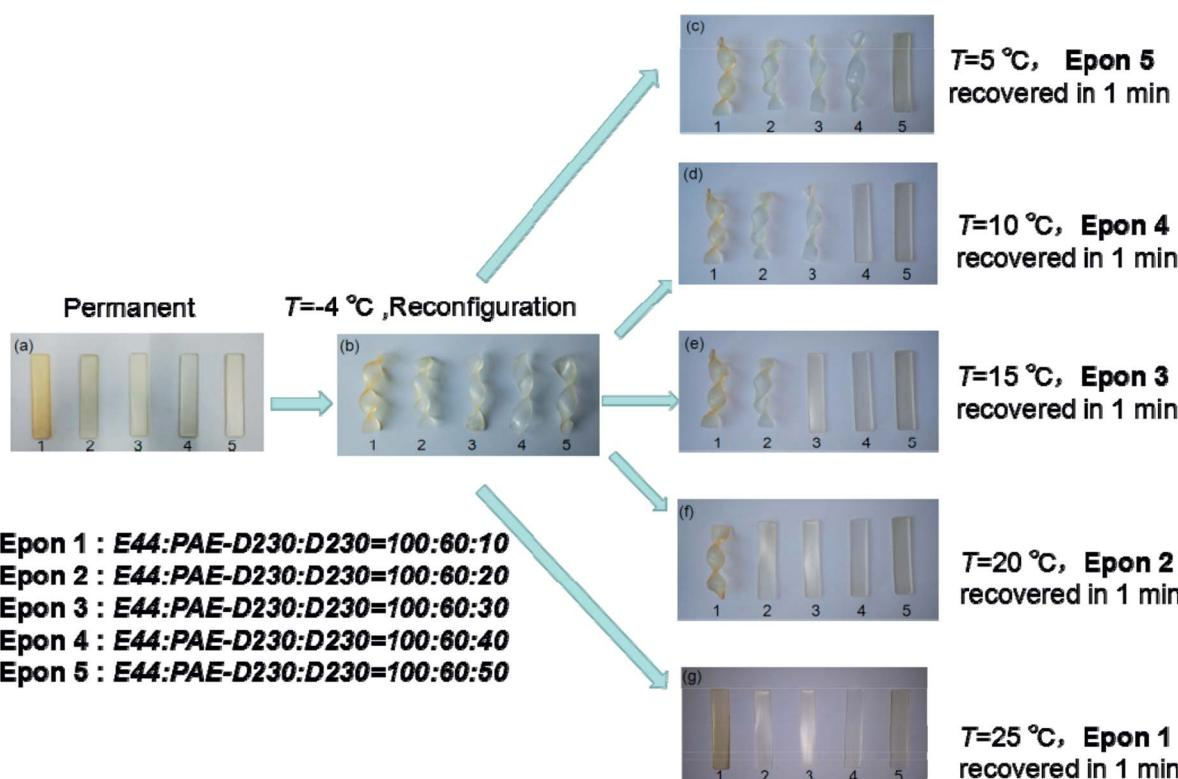


Fig. 7 Experiment of shape fixity and shape recovery.

samples, demonstrating excellent and tunable mechanical properties.

### 3.5 Shape memory behavior

To investigate the shape memory and reconfigurable properties, we did the following experiment. In this work, the shape memory behavior of the elastomers depends on their respective glass transition temperatures. Above their respective glass transition temperatures, the sample is in the rubbery state, and the elastomer can be shaped in a certain range. When the sample is below its respective glass transition temperatures, the movement of the segments is frozen, so the polymer shape is fixed until the temperature rises to their respective glass transition temperature, the movement of segments is activated again, and the sample shape will return to its original state. There were 5 typical samples (E44 : PAE-D230 : D230, 100 : 60 : 10–50) with various  $T_g$ s were deformed above their  $T_g$ s into twisted temporary shapes, then all samples were placed in  $-4^\circ\text{C}$  environment to fix twisted temporary shape as in Fig. 7a and b. When the sample was put in the water bath at the temperature of  $5^\circ\text{C}$ , the Epon 5 recovered in 1 min, the shape of the other samples did not change at all (Fig. 7c). Further immersion in  $10^\circ\text{C}$  water bath, Epon 4 recovered in 1 min (Fig. 7d), the shape of the other samples still did not change at all. Epon 3 recovered in 1 min at the temperature of  $15^\circ\text{C}$  and Epon 2 also recovered in 1 min at the temperature of  $20^\circ\text{C}$  (Fig. 7e and f). When the temperature was raised to  $25^\circ\text{C}$ , all the samples had recovered to the rectangular original shapes (Fig. 7g), indicating the successful preparation of epoxy based shape memory elastomers.

## 4. Conclusions

This work presented a facile preparation of epoxy based elastomers with tunable  $T_g$ s and mechanical properties. A secondary amine-capped polyaspartic ester (PAE-D230) was synthesized using diethyl maleate and amine-terminated polyether (D230) via Michael addition reaction. By modulating the molar ratio of preliminary amine containing D230 and secondary amine-capped PAE-D230 during the curing process with epoxy precursor E44, we obtained epoxy shape memory polymer with tunable  $T_g$ s ( $-12$ – $20^\circ\text{C}$ ), controllable mechanical properties with tensile stress from 0.8 to 14.1 MPa, tensile modulus from 0.7 to 872.0 MPa, and elongation at break from 45.2 to 195.1%. These facile tunable mechanical and  $T_g$ s properties illustrated the potential applications of these thermally induced shape-memory thermoplastics in actuators and biomedical field.

## Conflicts of interest

There are no conflicts to declare.

## Acknowledgements

This research is financially supported by “One Hundred Talented People” of the Chinese Academy of Sciences (Y60707WR04); National Basic Research Program (973 Program 2015CB654705); Zhejiang Provincial foundation of Natural Science (LY16B040004).

## References

- 1 M. Fache, C. Montérémal, B. Boutevin and S. Caillol, *Eur. Polym. J.*, 2015, **73**, 344–362.
- 2 J. Xin, P. Zhang, K. Huang and J. Zhang, *RSC Adv.*, 2014, **4**, 8525–8532.
- 3 X. Fernández-Francos, A. O. Konuray, A. Belmonte, S. D. L. Flor, A. Serra and X. Ramis, *Polym. Chem.*, 2016, **7**, 2280–2290.
- 4 I. Hamerton, B. J. Howlin, J. R. Jones, S. Liu and J. M. Barton, *J. Mater. Chem.*, 1996, **6**, 305–310.
- 5 Y. Huang, Y. Tian, Y. Li, X. Tan, Q. Li, J. Cheng and J. Zhang, *RSC Adv.*, 2017, **7**, 49074–49082.
- 6 Y. Tian, X. Zhang, H. Z. Geng, H. J. Yang, C. Li, S. X. Da, X. Lu, J. Wang and S. L. Jia, *RSC Adv.*, 2017, **7**, 53018–53024.
- 7 A. V. Rajulu, G. B. Rao, R. L. Reddy and R. Sanjeevi, *J. Reinf. Plast. Compos.*, 2010, **20**, 335–340.
- 8 J. T. Shen, S. T. Buschhorn, J. T. M. D. Hosson, K. Schulte and B. Fiedler, *Compos. Sci. Technol.*, 2015, **115**, 1–8.
- 9 J. P. Yang, Q. P. Feng, Z. K. Chen and S. Y. Fu, *J. Appl. Polym. Sci.*, 2011, **119**, 863–870.
- 10 X. Yang, C. Wang, S. Li, K. Huang, M. Li, W. Mao, S. Cao and J. Xia, *RSC Adv.*, 2016, **7**, 238–247.
- 11 J. Leng, F. Xie, X. Wu and Y. Liu, *J. Intell. Mater. Syst. Struct.*, 2014, **25**, 1256–1263.
- 12 G. P. Tandon, K. Goecke, K. Cable and J. Baur, *J. Intell. Mater. Syst. Struct.*, 2009, **20**, 2127–2143.
- 13 A. Arnebold and A. Hartwig, *Polymer*, 2016, **83**, 40–49.
- 14 R. Sujithra, S. M. Srinivasan and A. Arockiarajan, *Polym. Test.*, 2015, **48**, 1–6.
- 15 B. Zhou, X. L. Wu, Y. J. Liu and J. S. Leng, *Adv. Mater. Sci. Res.*, 2011, **179–180**, 325–328.
- 16 Y. L. Xiong, R. M. Wang, G. Zheng and L. U. Min-Fei, *China Adhes.*, 2005, **14**, 27–32.
- 17 Kavitha, A. Revathi, S. Rao, S. Srihari and G. N. Dayananda, *J. Polym. Res.*, 2012, **19**, 1–7.
- 18 M. Fan, J. Liu, X. Li, J. Cheng and J. Zhang, *Thermochim. Acta*, 2013, **554**, 39–47.
- 19 M. Fan, J. Liu, X. Li, J. Zhang and J. Cheng, *J. Polym. Res.*, 2014, **21**, 1–8.
- 20 T. Xie and I. A. Rousseau, *Polymer*, 2009, **50**, 1852–1856.
- 21 A. B. Leonardi, L. A. Fasce, I. A. Zucchi, C. E. Hoppe, E. R. Soulé, C. J. Pérez and R. J. J. Williams, *Eur. Polym. J.*, 2011, **47**, 362–369.
- 22 N. Zheng, G. Fang, Z. Cao, Q. Zhao and T. Xie, *Polym. Chem.*, 2015, **6**, 3046–3053.
- 23 A. Pyymaki Perros, H. Hakola, T. Sajavaara, T. Huhtio and H. Lipsanen, *J. Phys. D: Appl. Phys.*, 2013, **46**, 5502.



24 P. D. Tatiya, R. K. Hedaoo, P. P. Mahulikar and V. V. Gite, *Ind. Eng. Chem. Res.*, 2013, **52**, 1562–1570.

25 F. Fraga and E. R. Núñez, *J. Appl. Polym. Sci.*, 2015, **80**, 776–782.

26 F. Fraga and E. R. Núñez, *J. Appl. Polym. Sci.*, 2010, **82**, 461–466.

27 F. Fraga and E. R. Núñez, *J. Appl. Polym. Sci.*, 2010, **83**, 1692–1696.

28 L. Barral, J. Cano, J. López, I. López-Bueno, P. Nogueira, C. Ramírez and M. J. Abad, *J. Therm. Anal. Calorim.*, 1999, **55**, 37–45.

29 M. Arasa, X. Ramis, J. M. Salla, A. Mantecón and A. Serra, *Polym. Degrad. Stab.*, 2007, **92**, 2214–2222.

30 P. Sivasamy, M. Palaniandavar, C. T. Vijayakumar and K. Lederer, *Polym. Degrad. Stab.*, 1992, **38**, 15–21.

31 X. Fernández-Francos, J. M. Salla, A. Cadenato, J. M. Moráncho, A. Serra, A. Mantecón and X. Ramis, *J. Appl. Polym. Sci.*, 2009, **111**, 2822–2929.

32 L. Barral, J. Cano, J. López, I. López-Bueno, P. Nogueira, M. J. Abad and C. Ramírez, *Eur. Polym. J.*, 2000, **36**, 1231–1240.

33 S. Pooja, C. Veena and N. A. Kumar, *J. Appl. Polym. Sci.*, 2010, **107**, 1946–1953.

